

Multilevel Optical Systems With MLSD Receivers Insensitive to GVD and PMD

Giulio Colavolpe, *Member, IEEE*, Tommaso Foggi, Enrico Forestieri, *Member, IEEE*, and Giancarlo Prati, *Fellow, IEEE*

Abstract—This paper analyzes optical transmission systems based on high-order modulations such as phase-shift keying signals and quadrature amplitude modulations. When the channel is affected by group velocity dispersion (GVD), polarization mode dispersion (PMD), and phase uncertainties due to the laser phase noise, the optimal receiver processing based on maximum-likelihood sequence detection and its practical implementation through a Viterbi processor is described without a specific constraint on the receiver front end. The implementation issues are then faced, showing that at least a couple of widely known front ends, with proper modifications, can be used to extract the required sufficient statistics from the received signal. The aspects related to the receiver adaptivity, the complexity reduction of the Viterbi processor, and the possibility of employing polarization diversity at the transmitter end are also discussed. It is demonstrated that, as long as a sufficient number of Viterbi processor trellis states is employed, GVD and PMD entail no performance degradation with respect to the case of no channel distortions (the back-to-back case).

Index Terms—Differential encoding, electrical equalization, group velocity dispersion (GVD), intersymbol interference (ISI), maximum-likelihood sequence detection (MLSD), optical transmission systems, phase-shift keying (PSK), polarization mode dispersion (PMD), quadrature amplitude modulation (QAM), Viterbi algorithm (VA).

I. INTRODUCTION

THE ever-increasing transmission rate in optical systems determines a more severe impact of polarization mode dispersion (PMD) and group velocity dispersion (GVD) on the system performance. Optical compensation techniques have been proposed in the past but, although they are very effective, the need for advanced and high-cost technologies limits their development and use. Hence, a great interest in electrical equalization schemes, and, in particular, in schemes based on maximum-likelihood sequence detection (MLSD) [1], has arisen because of the possibility of exploiting simple, low-cost, and well-known solutions. However, a main result for intensity modulation with direct detection (IM/DD) schemes is that, although an MLSD receiver outperforms other electronic equalization techniques, its effectiveness in mitigating the effects of GVD and PMD is still far from that obtainable by optical compensation (see [2] and references therein). This is

due to the highly suboptimal front end processing based on a nonlinear device such as the photodetector.

Multilevel signaling formats based on amplitude modulations have been investigated in [3] and, more recently, other schemes, still based on multilevel modulations, have been proposed or have been brought back to the attention of the scientific community. In particular, we are referring to systems using differentially encoded quaternary phase-shift keying (QPSK) signals demodulated by an interferometric IM/DD receiver, recently proposed in [4] (see also [5] and references therein) and extended to higher order modulations in [6] and [7], or to systems using combined amplitude-phase modulations demodulated by coherent techniques [8], [9]. In both cases, the use of multilevel modulations allows to reduce, for a given bit rate, the signaling rate, thus reducing the impact of GVD and PMD. In addition, the use of a different and more sophisticated (with respect to a simple photodetector) front end gives hope that with a proper electronic processing the impact of PMD and GVD can be completely mitigated. If this is certainly true when synchronous coherent techniques are employed [8], [9], in the case of interferometric IM/DD receivers, some attempts to devise a more effective electronic processing are described in [10]–[12] where, by resorting to *multisymbol differential detection* methods, commonly adopted in wireless communications [13]–[15], the authors try to improve the performance over the conventional symbol-by-symbol receiver.

In this paper, we discuss the use of high-order modulations in optical transmission systems. First of all, without constraints on the receiver front end, we identify the optimal processing to be performed on the received signal from a theoretical point of view, showing that this optimal processing is able to perfectly compensate for PMD and GVD. The implementation aspects are then discussed, focusing on a couple of solutions based on the Viterbi algorithm (VA). Our results represent an evolution of those in [16] and [17] which in turn evolve from the multisymbol differential schemes in [13]–[15] (see [16] for a comprehensive discussion and performance comparison among these receivers). The state-complexity reduction of the VA is then described along with other side (although very important) aspects such as the channel estimation and the generalization to different channel encoders. The possibility of employing the described detection schemes in the case of *transmit* polarization diversity (often referred to as *polarization multiplexing*), hence further reducing the signaling rate for a given bit rate, will be also discussed. Regarding the receiver front end, it will be shown that we can employ either a (slightly modified) interferometric IM/DD front end, or a coherent front end, both homodyne and heterodyne. Although the proposed receivers allow

Manuscript received May 31, 2007. This work was supported in part by Ericsson and in part by the Italian Ministero dell'Istruzione, dell'Università e della Ricerca (MIUR), under the PRIN project STORiCo.

G. Colavolpe and T. Foggi are with University of Parma, Dipartimento di Ingegneria dell'Informazione, and the CNIT Research Unit, I-43100 Parma, Italy.

E. Forestieri and G. Prati are with Scuola Superiore Sant'Anna, I-56124 Pisa, Italy, and also with the Photonic Networks National Laboratory, CNIT, I-56124 Pisa, Italy.

Digital Object Identifier 10.1109/JLT.2008.917052

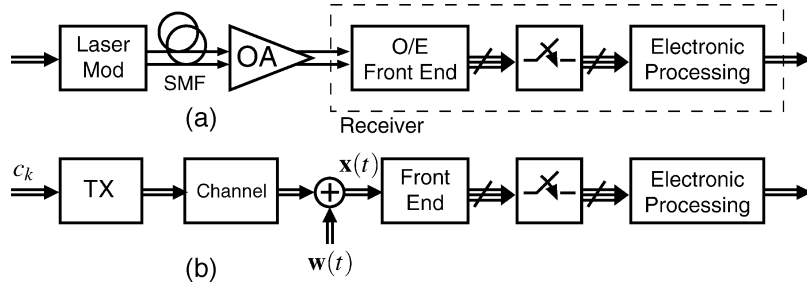


Fig. 1. (a) System model. (b) Low-pass equivalent.

for a perfect compensation of the dispersion effects when their complexity (in particular the number of the VA trellis states) is not constrained, in the numerical results we have also considered the effect of a limited receiver complexity on the system performance.

The paper is organized as follows. In Section II, the transmit signal is described along with the dispersion effects characterizing the channel propagation. The optimal receiver processing is analyzed in Section III, and its practical implementation through a Viterbi processor is discussed in Section IV. The possible receiver front ends are then described in Section V. Finally, in Section VI, the numerical results are shown, whereas in Section VII, some conclusions are drawn.

II. SYSTEM MODEL

The system model and its low-pass equivalent are shown in Fig. 1. In the considered system, a sequence $\mathbf{c} = (c_0, c_1, \dots, c_{K-1})^T$ of K complex symbols belonging to an M -ary complex alphabet \mathcal{C} is obtained, through a proper differential encoding rule [18], from a sequence $\mathbf{a} = (a_1, \dots, a_{K-1})^T$ of $K - 1$ complex symbols belonging to the same alphabet.¹ Without loss of generality, in the numerical results, we will consider classical phase-shift keying (PSK) signals, for which the standard differential encoding rule is employed, and square quadrature amplitude modulations (QAMs) for which quadrant differential encoding is adopted [18] (see also [16, Section V-A] for a concise description). However, our derivations can be also applied to other alphabets, for example amplitude- and phase-shift keying (APSK) modulations, whose signal constellations are composed of more concentric rings of PSK points.

After linear modulation, the signal is launched into a single-mode fiber (SMF) introducing PMD and GVD and is then optically amplified at the receiver end. We consider the receiver as composed of an analog part, the optoelectronic (O/E) front end, devoted to signal demodulation and conversion from the optical to the electrical domain, and a digital part devoted to electronic processing. The O/E front end may be based on interferometric IM/DD or coherent techniques, as explained later in Section V. The low-pass equivalent transfer function of a fiber affected by GVD only is $H_{\text{GVD}}(\omega) = \exp(-j\beta_2 L_f \omega^2/2)$, L_f being the fiber length and $\beta_2 = -\lambda_0 D/\omega_0$ the chromatic

dispersion parameter [19], where D is the fiber chromatic dispersion (usually expressed in ps/nm/km), and ω_0 and λ_0 the optical carrier frequency and wavelength, respectively. In a chromatic dispersion-compensated link, several pieces of fiber with alternating sign chromatic dispersion $D^{(i)}$ and appropriate length $L^{(i)}$ may be used and, as commonly done, we will indicate as residual dispersion the quantity $D_r = \sum_i D^{(i)} L^{(i)}$ in ps/nm. In order to make our results independent of the bit rate R_b , we will use the dimensionless chromatic dispersion index γ [20], defined as

$$\gamma = 2\lambda_0 R_b^2 D_r / \omega_0. \quad (1)$$

Using the chromatic dispersion index γ , the transfer function of a GVD compensated link can be written as $H_{\text{GVD}}(\omega) = \exp[j\gamma(\omega/R_b)^2/4]$. Accounting now for PMD, the fiber Jones matrix is written as $\mathbf{H}_f(\omega) = H_{\text{GVD}}(\omega)\mathbf{R}_2\mathbf{U}(\omega)\mathbf{R}_1$, where $\mathbf{U}(\omega)$ describes the fiber PMD on the basis of its principal states of polarization (PSPs) at the carrier frequency which, without loss of generality, can be taken to be coincident at the input and output. \mathbf{R}_1 and \mathbf{R}_2 are random rotation matrices, independent of frequency, representing a change of basis SOPs. A closed-form expression of $\mathbf{U}(\omega)$ accounting for all PMD orders is not known and although several second-order approximations are available (see [21] and references therein), they account differently for higher PMD orders [22]. To avoid the peculiarities of a specific analytical model, one could use the numerical random waveplate model.

Regarding the amplified spontaneous emission (ASE) noise, we assume that it is dominant over thermal and shot noise. Its low-pass equivalent is modeled as an additive white Gaussian noise (AWGN) $\mathbf{w}(t) = [w_1(t), w_2(t)]^T$, where $w_1(t)$ and $w_2(t)$ are independent complex noise components accounting for ASE on two orthogonal states of polarization (SOPs), each with two-sided power spectral density (PSD) equal to N_0 . The low-pass equivalent of the received signal is denoted by $\mathbf{x}(t) = [x_1(t), x_2(t)]^T$, being $x_1(t)$ and $x_2(t)$ the received signal components on the above mentioned orthogonal SOPs. We can express each component of $\mathbf{x}(t)$ as

$$x_i(t) = s_i(t, \mathbf{c})e^{j\theta_i(t)} + w_i(t), \quad i = 1, 2 \quad (2)$$

where $s_i(t, \mathbf{c})$ is the useful signal, distorted by GVD and PMD, and $\theta_i(t)$ is a time-varying phase uncertainty accounting for the

¹In the following, $(\cdot)^T$ denotes transpose, $(\cdot)^H$ transpose conjugate, and $(\cdot)^*$ complex conjugate

laser phase noise and for the uncertainties due to channel propagation. Although the source of phase noise is the same for both components, in general, $\theta_1(t)$ and $\theta_2(t)$ differ for an unknown phase shift, that we may assume uniformly distributed in the interval $[0, 2\pi)$. The useful signal components can be expressed as

$$s_i(t, \mathbf{c}) = \sum_{k=0}^{K-1} c_k p_i(t - kT), \quad i = 1, 2 \quad (3)$$

where $p_i(t)$ is the received pulse on the i th signal component and T the symbol interval. Without loss of generality, we may assume that the pulse $p_i(t)$ has its support in the interval $[0, (L_i + 1)T)$, where L_i is a suitable integer, and we will denote $L = \max_{i=1,2}\{L_i\}$. When $L \geq 1$, intersymbol interference (ISI) arises. Although, in general, the ISI causes a performance degradation [1], this is not the case of GVD and PMD. In fact, since the fiber Jones transfer matrix $\mathbf{H}_f(\omega)$ is unitary, it is $\mathbf{H}_f(\omega)\mathbf{H}_f^H(\omega) = \mathbf{H}_f(\omega)\mathbf{H}_f^{-1}(\omega) = \mathbf{I}$. Hence, the linear distortions introduced by a dispersive fiber, regarded as a two-input/two-output system, can be considered as the 2-D extension of what in a single input/single output system we call a ‘‘phase distortion.’’ This means that an ideal receiver could, in principle, estimate $\mathbf{H}_f(\omega)$ and filter the received signal with $\mathbf{H}_f^{-1}(f) = \mathbf{H}_f^H(f)$, thus perfectly compensating the distortions introduced by the channel, without modifying the noise statistics. Hence, the performance in the absence of distortions (the back-to-back case) could be attained. However, although the channel estimate is in general feasible, since GVD is a static phenomenon and PMD is slowly-varying, the implementation of the inverse filter² poses some complexity issues. In addition, when the phase noise is rapidly-varying, its estimate is not so trivial. In order to circumvent these problems, in the next sections we show an equivalent electronic processing and discuss its implementation aspects.

III. OPTIMAL RECEIVER PROCESSING

Not considering for now the implementation aspects of the receiver front end, a possible way of extracting sufficient statistics from the received signal $\mathbf{x}(t)$ is by means of proper analog prefiltering and sampling at the Nyquist rate [24]. In the following, we will assume that η samples per symbol interval are extracted from the signal. This number of samples depends on the bandwidth of the received useful signal. As an example, when its low-pass equivalent has a bandwidth $B_s \leq 1/2T$, $\eta = 1$ is sufficient, when $1/2T < B_s \leq 1/T$, $\eta = 2$ is sufficient, and so on. Without loss of generality, we assume that the analog prefilter has no effect on the useful signal and that its low-pass equivalent has a vestigial symmetry around $\eta/2T$ [24]. This latter condition ensures that the noise samples are independent and identically distributed complex Gaussian random variables with mean zero and variance $\sigma^2 = N_0\eta/T$ [24]. Denoting by $\mathbf{x}'(t) = [x'_1(t), x'_2(t)]^T$ and $\mathbf{w}'(t) = [w'_1(t), w'_2(t)]^T$,

²The inverse filter can be approximated by an optical compensator (e.g., see [23] and references therein).

the received signal and noise after the analog prefilter, we define ($i = 1, 2, k = 0, 1, \dots, K-1, n = 0, 1, \dots, \eta-1$)

$$\begin{aligned} x_{i,k\eta+n} &\triangleq x'_i(kT + nT_c) \\ s_{i,k\eta+n}(\mathbf{c}) &\triangleq s_i(kT + nT_c, \mathbf{c}) \\ \theta_{i,k\eta+n} &\triangleq \theta_i(kT + nT_c) \\ w_{i,k\eta+n} &\triangleq w'_i(kT + nT_c) \end{aligned} \quad (4)$$

where $T_c = T/\eta$ is the sampling interval. Due to the limited support of the pulse $p_i(t)$, it is $s_{i,k\eta+n}(\mathbf{c}) = s_{i,k\eta+n}(\mathbf{c}_{k-L_i}^k)$.³ From (2) and (3), we have

$$\begin{aligned} x_{i,k\eta+n} &= s_{i,k\eta+n}(\mathbf{c}_{k-L_i}^k) e^{j\theta_{i,k\eta+n}} + w_{i,k\eta+n} \\ &= \sum_{\ell=0}^{L_i} c_{k-\ell} p_i(\ell T + nT_c) e^{j\theta_{i,k\eta+n}} + w_{i,k\eta+n}. \end{aligned} \quad (5)$$

Let us define $\mathbf{p}_{i,n} = [p_i(nT_c), p_i(T + nT_c), \dots, p_i(L_i T + nT_c)]^T$, $i = 1, 2, n = 0, 1, \dots, \eta-1$. Assuming for the moment that the phase noise is constant during the whole transmission, i.e., $\theta_i(t) = \theta_i$, with θ_i modeled as a random variable uniformly distributed in the interval $[0, 2\pi)$, and that vectors $\mathbf{p}_{i,n}$ are perfectly known to the receiver, the sequence $\hat{\mathbf{c}}$, detected according to the MLSD strategy, can be expressed as

$$\hat{\mathbf{c}} = \arg \max_{\mathbf{c}} \Lambda(\mathbf{c}) \quad (6)$$

where the sequence metric $\Lambda(\mathbf{c})$ has the expression

$$\begin{aligned} \Lambda(\mathbf{c}) &= \sum_{i=1}^2 \left[\left| \sum_{k=0}^{K-1} \sum_{n=0}^{\eta-1} x_{i,k\eta+n} s_{i,k\eta+n}^* (\mathbf{c}_{k-L_i}^k) \right| \right. \\ &\quad \left. - \frac{1}{2} \sum_{k=0}^{K-1} \sum_{n=0}^{\eta-1} |s_{i,k\eta+n}(\mathbf{c}_{k-L_i}^k)|^2 \right]. \end{aligned} \quad (7)$$

This strategy is an extension of that in [16, eqn. (18)] to the case of multiple samples per symbol interval and of two received signals which, conditionally to the sequence \mathbf{c} , are independent. In addition, the approximation $\ln I_0(x) \simeq x$, where $I_0(x)$ is the zero-th order modified Bessel function of the first kind, has been used and the terms irrelevant for the detection process have been discarded.

As demonstrated by means of information theory arguments [25]–[27], the strategy (6), (7) attains the same performance of the ideal receiver which perfectly knows the channel phases θ_i in addition to vectors $\mathbf{p}_{i,n}$. Hence, this receiver as well is insensitive to phase distortions as PMD and GVD. Unfortunately, there are a few problems related to the implementation of the strategy (6), (7). By means of the same manipulations described in [16], the sequence metric $\Lambda(\mathbf{c})$ can be equivalently computed as

$$\Lambda(\mathbf{c}) = \sum_{k=0}^{K-1} \Delta_k(\mathbf{c}_0^k) \quad (8)$$

³In the following, given two integers k_1 and $k_2 > k_1$, we define $\mathbf{c}_{k_1}^{k_2} \triangleq (c_{k_1}, c_{k_1+1}, \dots, c_{k_2})^T$. Obviously, $\mathbf{c} = \mathbf{c}_0^{K-1}$.

where

$$\Delta_k(\mathbf{c}_0^k) = \sum_{i=1}^2 \left[\left| \sum_{n=0}^{\eta-1} x_{i,k\eta+n} s_{i,k\eta+n}^* (\mathbf{c}_{k-L_i}^k) + q_{i,k-1}(\mathbf{c}_0^{k-1}) \right| - \left| q_{i,k-1}(\mathbf{c}_0^{k-1}) \right| - \frac{1}{2} \sum_{n=0}^{\eta-1} |s_{i,k\eta+n}(\mathbf{c}_{k-L_i}^k)|^2 \right] \quad (9)$$

and

$$q_{i,k-1}(\mathbf{c}_0^{k-1}) = \sum_{m=0}^{k-1} \sum_{n=0}^{\eta-1} x_{i,m\eta+n} s_{i,m\eta+n}^* (\mathbf{c}_{m-L_i}^m). \quad (10)$$

The difficulty inherent in the incremental metric (9) is its unlimited memory. In fact, $\Delta_k(\mathbf{c}_0^k)$ depends on the entire previous code sequence [16]. This implies that the maximization of the sequence metric cannot be implemented by means of the VA working on a properly defined trellis diagram [28].

Other problems must be also considered. Indeed, in order to obtain the MLSD strategy (6), (7), constant channel phases θ_i and perfectly known vectors $\mathbf{p}_{i,n}$ have been assumed. These problems will be faced in the next section.

IV. PRACTICAL IMPLEMENTATION

A. Rectangular Window

A possible solution for the above mentioned problem of unlimited memory of the incremental metric $\Delta_k(\mathbf{c}_0^k)$ in (9) is suggested in [16], where it is proposed to truncate $q_{i,k-1}(\mathbf{c}_0^{k-1})$ by using a rectangular window. In other words, $q_{i,k-1}(\mathbf{c}_0^{k-1})$ in (10) is substituted by

$$q_{i,k-1}^{(N)}(\mathbf{c}_{k-N-L_i}^{k-1}) = \sum_{m=k-N}^{k-1} \sum_{n=0}^{\eta-1} x_{i,m\eta+n} s_{i,m\eta+n}^* (\mathbf{c}_{m-L_i}^m). \quad (11)$$

The design integer parameter N is called *implicit phase memory* [16]. The resulting sequence metric can be approximated as

$$\Lambda(\mathbf{c}) \simeq \sum_{k=0}^{K-1} \lambda_k^{(N)}(\mathbf{c}_{k-N-L_i}^k) \quad (12)$$

with

$$\lambda_k^{(N)}(\mathbf{c}_{k-N-L_i}^k) = \sum_{i=1}^2 \left[\left| \sum_{n=0}^{\eta-1} x_{i,k\eta+n} s_{i,k\eta+n}^* (\mathbf{c}_{k-L_i}^k) + q_{i,k-1}^{(N)}(\mathbf{c}_{k-N-L_i}^{k-1}) \right| - \left| q_{i,k-1}^{(N)}(\mathbf{c}_{k-N-L_i}^{k-1}) \right| - \frac{1}{2} \sum_{n=0}^{\eta-1} |s_{i,k\eta+n}(\mathbf{c}_{k-L_i}^k)|^2 \right]. \quad (13)$$

In this case, the maximization of the approximated sequence metric (12) can be performed by means of the VA and $\lambda_k^{(N)}(\mathbf{c}_{k-N-L_i}^k)$ assumes the meaning of branch metric on a trellis diagram whose state is defined as $\mu_k^{(N)} = \mathbf{c}_{k-N-L_i}^{k-1}$.

Hence, the number of states depends exponentially on $L + N$. However, techniques for state-complexity reduction, such as those described in Section IV-C, can be used in order to limit the number of states without excessively reducing the value of N .

In the case of constant channel phases θ_i , although in principle the performance of the optimal detection strategy (6), (7) is obtained only when $N \rightarrow \infty$ [29], it is sufficient to use small values of N (a few units) to obtain a performance very close to the optimal one [16]. On the other hand, this new algorithm requires approximately constant channel phases θ_i in a window of N symbol intervals only [16]. Hence, it can be used when the channel phases are time-varying—the smaller the value of N , the greater the robustness to the phase noise. Finally, from (13), notice that, although more samples per symbol interval are used as a sufficient statistic, the VA works at the symbol rate.

B. Exponential Window

Instead of a rectangular window, in [17], an exponentially decaying window is employed. In particular, a trellis state $\mu_k = \mathbf{c}_{k-L}^{k-1}$ is defined and $q_{i,k-1}(\mathbf{c}_0^{k-1})$ in (10) is substituted by a complex quantity $q_{i,k-1}^{(\alpha)}(\mu_k)$ estimated based on per-survivor processing [30] and computed recursively as

$$q_{i,k-1}^{(\alpha)}(\mu_k) = \alpha q_{i,k-2}^{(\alpha)}(\mu_{k-1}) + \sum_{n=0}^{\eta-1} x_{i,(k-1)\eta+n} s_{i,(k-1)\eta+n}^* (\mathbf{c}_{k-1-L_i}^{k-1}) \quad (14)$$

where $0 \leq \alpha \leq 1$ is a *forgetting factor*. Therefore, the resulting sequence metric is

$$\Lambda(\mathbf{c}) \simeq \sum_{k=0}^{K-1} \lambda_k^{(\alpha)}(c_k, \mu_k) \quad (15)$$

with

$$\begin{aligned} \lambda_k^{(\alpha)}(c_k, \mu_k) &= \lambda_k^{(\alpha)}(\mathbf{c}_{k-L}^k) \\ &= \sum_{i=1}^2 \left[\left| \sum_{n=0}^{\eta-1} x_{i,k\eta+n} s_{i,k\eta+n}^* (\mathbf{c}_{k-L_i}^k) + q_{i,k-1}^{(\alpha)}(\mu_k) \right| - \left| q_{i,k-1}^{(\alpha)}(\mu_k) \right| - \frac{1}{2} \sum_{n=0}^{\eta-1} |s_{i,k\eta+n}(\mathbf{c}_{k-L_i}^k)|^2 \right] \end{aligned} \quad (16)$$

and its maximization is performed by means of the VA working at a symbol rate. When the channel phases are constant, for $\alpha \rightarrow 1$ the performance of this algorithm tends to that of the optimal one [17], hence ensuring in this case no performance degradation due to PMD and GVD, too. In addition, this algorithm also works well in the presence of a time-varying phase noise, although it is less robust than that described in Section IV-A. To this purpose, the value of α must be optimized for the phase noise at hand. Since for the phase noise of the commonly used lasers the robustness of this algorithm is sufficient, in the numerical results, we will only consider it.

We would like to point out a different equivalent expression for the branch metric (16). To illustrate the main idea, we limit

ourself to the case $\eta = 2$ that will be considered in the numerical results. The branch metric (16) can be expressed as

$$\begin{aligned} \lambda_k^{(\alpha)}(c_k, \mu_k) &= \sum_{i=1}^2 \left\{ \frac{1}{|x_{i,2k}|} \left[|x_{i,2k}^* x_{i,2k+1} s_{i,2k+1}^* (c_{k-L_i}^k) \right. \right. \\ &\quad \left. \left. + |x_{i,2k}|^2 s_{i,2k}^* (c_{k-L_i}^k) + x_{i,2k}^* q_{i,k-1}^{(\alpha)}(\mu_k) \right] \right. \\ &\quad \left. - \left[x_{i,2k}^* q_{i,k-1}^{(\alpha)}(\mu_k) \right] \right\} \\ &\quad - \frac{1}{2} |s_{i,2k+1}(c_{k-L_i}^k)|^2 - \frac{1}{2} |s_{i,2k}(c_{k-L_i}^k)|^2 \} \quad (17) \end{aligned}$$

with

$$q_{i,k-1}^{(\alpha)}(\mu_k) = \alpha q_{i,k-2}^{(\alpha)}(\mu_{k-1}) + x_{i,2k-1} s_{i,2k-1}^* (c_{k-1-L_i}^{k-1}) + x_{i,2k-2} s_{i,2k-2}^* (c_{k-1-L_i}^{k-1}).$$

Defining now

$$z_{i,\ell} \triangleq x_{i,\ell} x_{i,\ell-1}^* \quad (18)$$

and taking into account that

$$x_{i,\ell} x_{i,\ell-2}^* = \frac{z_{i,\ell} z_{i,\ell-1}}{|x_{i,\ell-1}|^2} \quad (19)$$

we can express

$$\begin{aligned} \lambda_k^{(\alpha)}(c_{k-L}) &= \sum_{i=1}^2 \left\{ \frac{1}{|x_{i,2k}|} \left[|z_{i,2k+1} s_{i,2k+1}^* (c_{k-L_i}^k) \right. \right. \\ &\quad \left. \left. + |x_{i,2k}|^2 s_{i,2k}^* (c_{k-L_i}^k) + g_{i,k-1}^{(\alpha)}(\mu_k) \right] \right. \\ &\quad \left. - \left[g_{i,k-1}^{(\alpha)}(\mu_k) \right] - \frac{1}{2} |s_{i,2k+1}(c_{k-L_i}^k)|^2 \right. \\ &\quad \left. - \frac{1}{2} |s_{i,2k}(c_{k-L_i}^k)|^2 \right\} \quad (20) \end{aligned}$$

where $g_{i,k-1}^{(\alpha)}(\mu_k) \triangleq x_{i,2k}^* q_{i,k-1}^{(\alpha)}(\mu_k)$ can be computed recursively as

$$\begin{aligned} g_{i,k-1}^{(\alpha)}(\mu_k) &= \alpha g_{i,k-2}^{(\alpha)}(\mu_{k-1}) \frac{z_{i,2k}^* z_{i,2k-1}^*}{|x_{i,2k-1}|^2 |x_{i,2k-2}|^2} + z_{i,2k}^* s_{i,2k-1}^* \\ &\quad \times (c_{k-1-L_i}^{k-1}) + \frac{z_{i,2k}^* z_{i,2k-1}^*}{|x_{i,2k-1}|^2} s_{i,2k-2}^* (c_{k-1-L_i}^{k-1}). \quad (21) \end{aligned}$$

In other words, the branch metric can be equivalently computed by using samples $\{z_{i,k\eta+n}\}$ and $\{|x_{i,k\eta+n}|\}$ instead of samples $\{x_{i,k\eta+n}\}$. This equivalent expression will be exploited in an alternative receiver implementation described in Section V-B.

Similar considerations hold for the branch metric (13)—in this case as well, the branch metric can be expressed as a function of $\{z_{i,k\eta+n}\}$ and $\{|x_{i,k\eta+n}|\}$.

C. Complexity Reduction

The state-complexity of the detection schemes described in Sections IV-A and IV-B can be limited by employing the well-known reduced-state sequence detection (RSSD) technique [31]–[33]. Following this technique, a reduced number of symbols is considered in the trellis state definition, hence reducing the number of trellis states. More complex techniques based on set partitioning may also be employed [31]–[33].

In order to compute the branch metrics (13), (16), or (20) in the reduced trellis, the necessary symbols not included or not completely specified in the state definition may be found in the survivor history. We note that, in the limiting case of a degenerate trellis diagram with only one state, symbol-by-symbol detection with decision feedback is performed. By using the RSSD technique, the number of states becomes a degree of freedom to trade performance against complexity. As we will see in the numerical results, when the number of trellis states is lower than M^L , a performance loss must be expected.

D. Channel Estimation

The algorithms described in Sections IV-A and IV-B require the knowledge of vectors $\mathbf{p}_{i,n}$ up to a constant phase term. For this estimation problem, conventional least mean-square (LMS) and recursive least-squares (RLS) algorithms [1] cannot be employed [34]. However, the noncoherent LMS and RLS techniques proposed in [34] can be straightforwardly extended to this case of two conditionally independent received signals and multiple samples per symbol intervals. In addition, they prove to be very robust against phase variations.

Denoting by $\hat{\mathbf{p}}_{i,n}^{(k)}$ the estimate of vector $\mathbf{p}_{i,n}$ at the k th symbol interval and assuming, although not necessary since the PMD is a slowly-varying phenomenon, that this estimate is updated at each symbol interval, we now extend the update rule for the noncoherent LMS in [34] to our case. Without taking into account the decision delay of the VA, the channel estimate is updated as

$$\hat{\mathbf{p}}_{i,n}^{(k+1)} = \hat{\mathbf{p}}_{i,n}^{(k)} + \delta \left[\frac{q_{i,k}^{(\cdot)}}{|q_{i,k}^{(\cdot)}|} x_{i,k\eta+n}^* - s_{i,k\eta+n}^* (\hat{\mathbf{c}}_{k-L_i}^k) \right] \hat{\mathbf{c}}_{k-L_i}^k \quad (22)$$

where δ is the adaptation step-size and $q_{i,k}^{(\cdot)}$ can be either $q_{i,k}^{(N)}$ in (11) or $q_{i,k}^{(\alpha)}$ in (14). Since the VA provides decisions with a delay $3L \div 5L$, for rapidly varying channels tentative decisions [1] or per-survivor processing [30] are usually adopted. However, in this case of a slowly varying channel, the more reliable VA final decisions can be used without affecting the receiver performance.

It is worth mentioning that the recursive relation (22) to update the channel coefficients can be also equivalently expressed as a function of samples $\{z_{i,k\eta+n}\}$ and $\{|x_{i,k\eta+n}|\}$. As an example, in the case $\eta = 2$, we can express

$$\begin{aligned} \hat{\mathbf{p}}_{i,0}^{(k+1)} &= \hat{\mathbf{p}}_{i,0}^{(k)} \\ &\quad + \delta \left[\frac{g_{i,k}^{(\cdot)}}{|g_{i,k}^{(\cdot)}|} \frac{z_{i,2k+2} z_{i,2k+1}}{|x_{i,2k+2}| |x_{i,2k+1}|} - s_{i,2k}^* (\hat{\mathbf{c}}_{k-L_i}^k) \right] \hat{\mathbf{c}}_{k-L_i}^k \\ \hat{\mathbf{p}}_{i,1}^{(k+1)} &= \hat{\mathbf{p}}_{i,1}^{(k)} \\ &\quad + \delta \left[\frac{g_{i,k}^{(\cdot)}}{|g_{i,k}^{(\cdot)}|} \frac{z_{i,2k+2}}{|x_{i,2k+2}|} - s_{i,2k+1}^* (\hat{\mathbf{c}}_{k-L_i}^k) \right] \hat{\mathbf{c}}_{k-L_i}^k. \quad (23) \end{aligned}$$

E. Application to Different Channel Encoders

The receivers proposed in [16] and [17] represent a generalization, to larger observation windows and to modulation formats

other than M -ary PSK, of the classical differential receiver [1]. In addition, these receivers can be adopted to decode not only differentially encoded symbols but also more powerful channel coding schemes provided that they are *noncoherently noncatastrophic* or known symbols are inserted to remove the phase ambiguities [16]. The VA branch metric in this case remains unchanged.

The same branch metric can be used for the algorithm by Bahl, Cocke, Jelinek, and Raviv (BCJR) [35], implementing the MAP symbol detection strategy and employed as a component decoder in iterative decoding schemes for turbo codes [36], and also for message-passing algorithms used to decode low-density parity-check codes [37].

F. Polarization Multiplexing (or Transmit Polarization Diversity)

The receivers described so far process independently the signals on two orthogonal SOPs before the VA. The VA branch metric is then computed as a sum of two independent contributions, one for each SOP. In other words, polarization diversity is adopted at the receiver end. Obviously, this corresponds to doubling the receiver front end and we wonder whether it is possible to use this complexity increase in a more profitable way. That is to say whether polarization multiplexing (polMUX), or in other words transmit polarization diversity, can be also employed at the transmitter end in order to double the spectral efficiency while keeping the same receiver structure. The answer to this question is affirmative. In fact, the described receiver structure can be adopted “as is” in the case of two independent data sequences $\mathbf{c}^{(1)} = \{c_k^{(1)}\}$ and $\mathbf{c}^{(2)} = \{c_k^{(2)}\}$ transmitted on two orthogonal polarizations. A single VA with branch metrics (13) or (16) can still be adopted, the only difference being the fact that the signal terms appearing in the branch metrics are now $s_{i,k\eta+n}(\mathbf{c}_{k-L_i}^{(1)k}, \mathbf{c}_{k-L_i}^{(2)k})$, i.e., they are a function of symbols of both sequences. Hence, a supertrellis must be built taking into account both sequences. Provided that a sufficient number of trellis states is considered, the described receiver is able to separate both signals and compensate phase distortions as GVD and PMD with no performance loss.

V. POSSIBLE RECEIVER FRONT ENDS

Up until now, we described the proposed electronic processing taking no interest in the O/E front end. We will now show that at least a couple of front end families can be equivalently employed.

A. Coherent Front End

A first possible receiver front end is that used in *coherent systems* based on *homodyne* or *heterodyne* techniques [9].⁴ As illustrated in Fig. 2 for the homodyne case, after a preliminary op-

⁴There is some confusion between the terminology used in the optical community and that used in the context of wireless communication systems. In wireless systems, the term “coherent” refers to the knowledge of the phase of the received signal, that is a coherent receiver is designed assuming that the phase of the received signal is known or separately estimated. On the contrary, a non-coherent receiver is designed assuming that the channel phase is unknown and modeled as a random variable or a stochastic process. This terminology is employed in [16], [17], [25]–[27], [29], [34], [36], and [37]. In optical systems, the term “coherent” refers to the coherence of the optical carrier whereas the terms “synchronous” or “asynchronous” refer to a processing which assumes or not the knowledge of the channel phase.

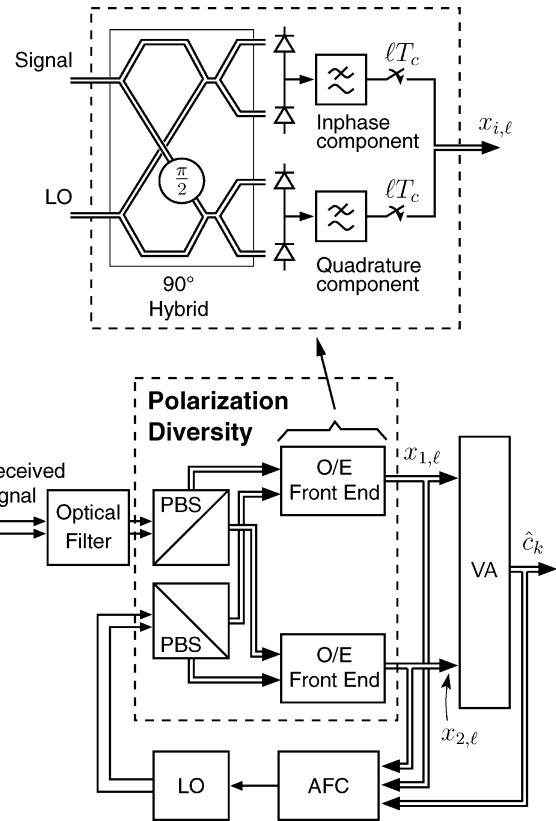


Fig. 2. Receiver using coherent homodyne detection.

tical filtering, two orthogonal SOPs are split through a polarization beam splitter (PBS). They are then separately combined with the optical field of a local oscillator laser (LO) in a 2×4 90° hybrid [8] and detected with two balanced photodetectors. In this way, the two received signals, one for each SOP, are converted in the electrical domain, in practice performing a frequency conversion. When the local-oscillator frequency coincides with that of the received signal, homodyne detection is performed. Otherwise, in heterodyne schemes a second frequency conversion stage in the electrical domain is necessary [8], [9].

Since the receivers described in the previous section do not require the knowledge of the channel phases θ_i , that is they represent two ways of performing asynchronous processing (with optimal performance), it is not necessary to track the channel phases with an optical (in the case of homodyne detection) or an electrical (in the case of heterodyne detection) phase-locked loop (PLL) but only the frequency must be tracked by an automatic frequency control (AFC), thus simplifying the receiver implementation. Regarding the analog prefiltering before sampling, mentioned in Section III, it can be performed either in the optical or in the electrical domain, in this latter case either at baseband or at intermediate frequency.

B. Interferometric IM/DD Front End

A (slightly modified) interferometric IM/DD front end, originally proposed in [4] for differentially encoded QPSK, can also be adopted. As already mentioned, due to the need of performing polarization diversity, the front end processing must be

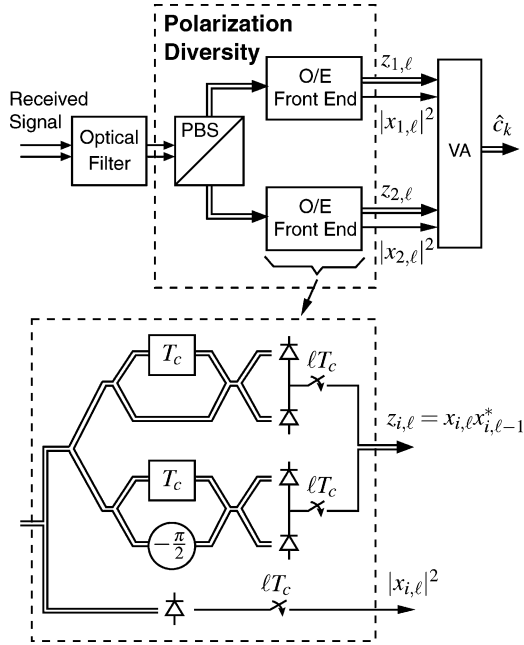


Fig. 3. Receiver using the interferometric IM/DD front end.

doubled. Hence, after the optical filter a PBS splits the signals on two orthogonal SOPs.

Given the signal on the i th SOP at the input of the interferometric IM/DD front end, the samples $\{z_{i,k\eta+n}\}$ are obtained at the output. As a consequence, an additional photodetector must be also employed to obtain the samples $\{|x_{i,k\eta+n}|^2\}$ which are necessary, along with samples $\{z_{i,k\eta+n}\}$, to compute the VA branch metric in the form (20). With respect to the interferometric IM/DD front end used in the receivers for differentially encoded QPSK, the delay is T_c and not T , whereas the phase shifts are 0 and $-\pi/2$ instead of $\pi/4$ and $-\pi/4$. This is because, at the sampling time ℓT_c , we want to obtain the output samples $\Re[z_{i,\ell}]$ and $\Re[e^{-j\pi/2}z_{i,\ell}] = \Im[z_{i,\ell}]$, instead of $\Re[e^{j\pi/4}z_{i,\ell}]$ and $\Re[e^{-j\pi/4}z_{i,\ell}]$. Notice that, in this case, the analog prefiltering before sampling, mentioned in Section III, must be performed in the optical domain. Hence, more attention must be devoted to the implementation of this filter. The overall receiver is shown in Fig. 3.

VI. NUMERICAL RESULTS

We performed standard Monte Carlo simulations to evaluate the performance of the proposed receivers. The considered modulation formats are QPSK and 8-PSK with the standard differential encoding rule and 16-QAM with quadrant differential encoding. Gray mapping is employed to map bits onto M -ary symbols.

A nonreturn-to-zero (NRZ) pulse filtered through an electrical baseband Gaussian filter with -3 dB bandwidth equal to $1/T$ is adopted at the transmitter. At the receiver, we use an optical fourth-order Gaussian filter with -3 dB bandwidth equal to $2/T$ and the described modified interferometric IM/DD front end, even though identical results would be obtained for example with the coherent (both homodyne and heterodyne, since they are equivalent in terms of performance when ASE noise dominates [38]) front end. Although the receive filter is only

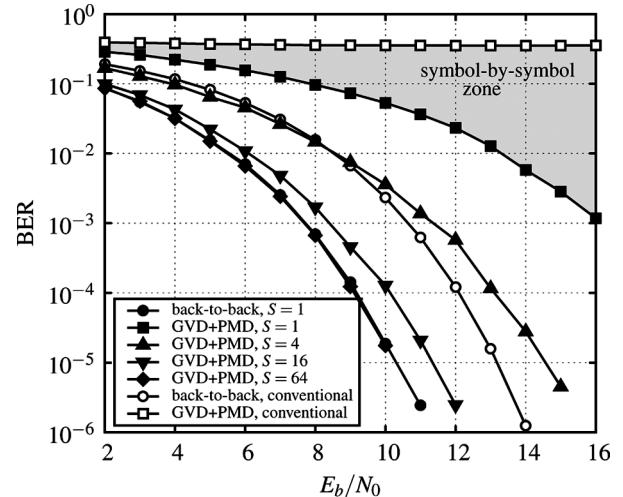


Fig. 4. Performance of the proposed algorithm for a QPSK transmission.

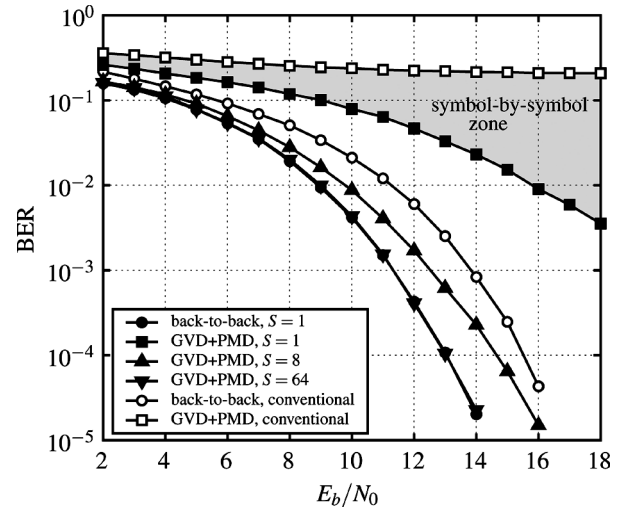


Fig. 5. Performance of the proposed algorithm for an 8-PSK transmission.

an approximation of the ideal analog prefilter, we verified that the related performance loss is less than one-tenth of a decibel. The receiver works using two samples per symbol interval and is based on the branch metrics (20). When employed, channel estimation is based on the updating rules (23).

In Figs. 4–7, we show bit-error ratio (BER) curves versus E_b/N_0 , E_b being the received signal energy per information bit. In all these figures, the presence of GVD, second-order PMD, and phase noise is considered. As already mentioned, GVD is characterized by a single parameter γ . As regards second-order PMD, it can be characterized by the values of the signal power splitting ρ among the PSPs, the differential group delay (DGD) τ , the DGD derivative $\Delta\tau_\omega$, and the PSPs rotation rate q_ω . Finally, phase noise can be characterized by its linewidth $\Delta\nu/T_b$ normalized to the bit rate. In the reported BER results, the following values are considered: $\gamma = 1.6$, $\rho = 0.5$, $\Delta\tau = 3T_b$, $\Delta\tau_\omega = 0.4T_b^2$, $q_\omega = 0.4T_b$, and $\Delta\nu/T_b = 0.25 \cdot 10^{-4}$, corresponding to $\Delta\nu = 1$ MHz for a bit rate $1/T_b = 40$ Gb/s.

In Fig. 4, QPSK is considered. The performance of the proposed algorithm is shown for a different number of trellis states. Indeed, thanks to the RSSD technique this value can be chosen

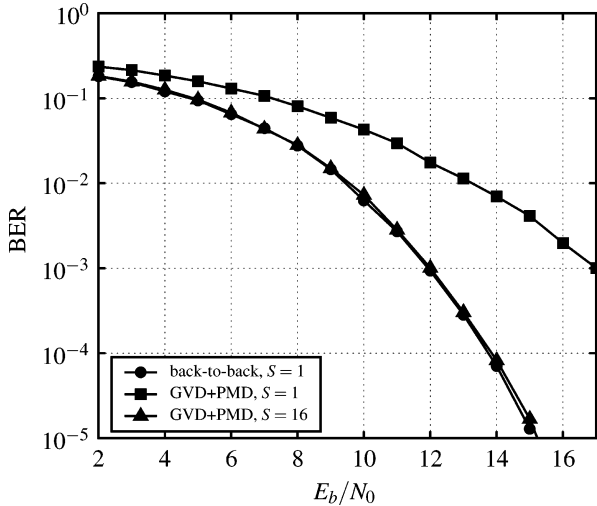


Fig. 6. Performance of the proposed algorithm for a 16-QAM transmission.

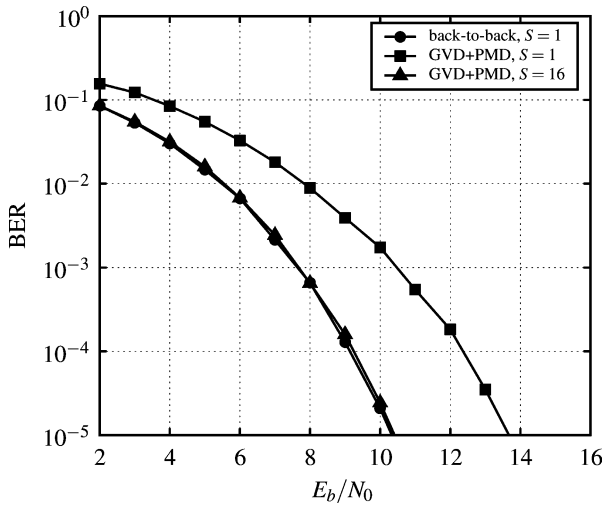


Fig. 7. Performance of the proposed algorithm for a QPSK transmission with transmit polarization diversity.

arbitrarily. Note that $S = 1$ means that a symbol-by-symbol receiver with decision feedback is considered. Although the channel estimation algorithm is employed in a completely blind manner (that is no training symbols are used in the acquisition phase), no perceptible difference has been observed with respect to the case of perfect knowledge of the received pulse. For this reason, in the remaining figures a perfect knowledge of the channel is assumed. As a comparison, the performance of the proposed algorithm in the absence of GVD and PMD (the back-to-back case) and that of the conventional symbol-by-symbol receiver [4] in the absence and in the presence of GVD and PMD are also shown. Note that in the back-to-back case the amount of ISI is very limited. As a consequence, the proposed receiver with $S = 1$ (solid circles) practically attains the optimal performance. Also note that with respect to the conventional receiver (hollow circles), the proposed algorithm exhibits a gain of more than 2 dB in the back-to-back case. This is in line with the results in [16]. In addition, in the presence of GVD and PMD, the performance of the conventional receiver rapidly degrades whereas the

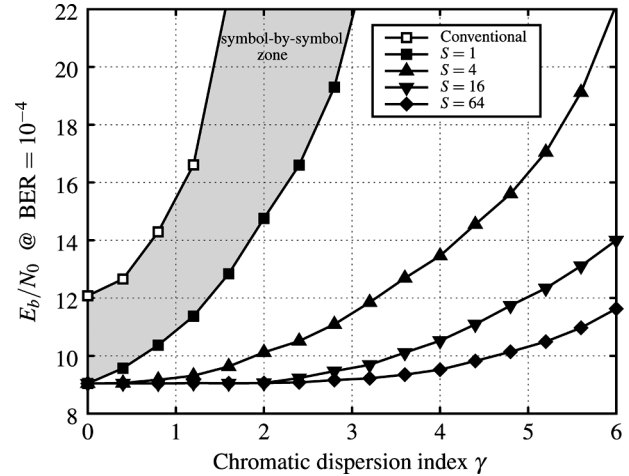


Fig. 8. Values of E_b/N_0 necessary to obtain a BER of 10^{-4} versus the value of γ , when GVD only is present. The considered modulation format is a QPSK.

proposed algorithm is able to perfectly compensate for both PMD and GVD, provided that a sufficient number of trellis states is adopted. As already mentioned, the proposed receiver with $S = 1$ is a symbol-by-symbol receiver with decision feedback. This can be considered as the best nonlinear decision feedback equalizer we can design, at least in the case of the interferometric front end. Hence, in the presence of GVD and second-order PMD with the described parameters, the region between the curves with solid and hollow squares represents the “symbol-by-symbol zone,” that is no matter what electronic processing is used, when we do not employ the VA, the performance curve will fall in that zone.

Similar considerations hold for the 8-PSK and the 16-QAM formats considered in Fig. 5 and Fig. 6, respectively. In the 16-QAM case, a conventional receiver is not defined, so no comparison is performed.

Fig. 7 deserves a more detailed comment. In this case, we consider a QPSK transmission with transmit polarization diversity and we show the overall BER performance. As can be seen, provided that a sufficient number of states is adopted, the performance of the back-to-back case, which coincides with that in Fig. 4, can be attained. This means that the proposed receiver is not only able to perfectly compensate PMD and GVD but is also able to separate both signals.

To assess the robustness to GVD and PMD of the proposed schemes with limited complexity, in Figs. 8 and 9, we show, for the QPSK modulation, the values of E_b/N_0 necessary to obtain a BER of 10^{-4} for a different amount of dispersion. In Fig. 8, the presence of GVD only is considered. On the contrary, in Fig. 9, only first-order PMD, with $\rho = 0.5$ and different values of $\Delta\tau$, is present. The robustness of the conventional receiver is also shown. The proposed receiver, even in a symbol-by-symbol configuration ($S = 1$), is able to guarantee a significant performance improvement with respect to the conventional one. In addition, by increasing the number of trellis states of the VA, the robustness is greatly increased. It is worth mentioning the particular behavior in the presence of first-order PMD. In fact, it can be observed that, when the VA trellis complexity is not sufficient to guarantee a perfect compensation, the performance

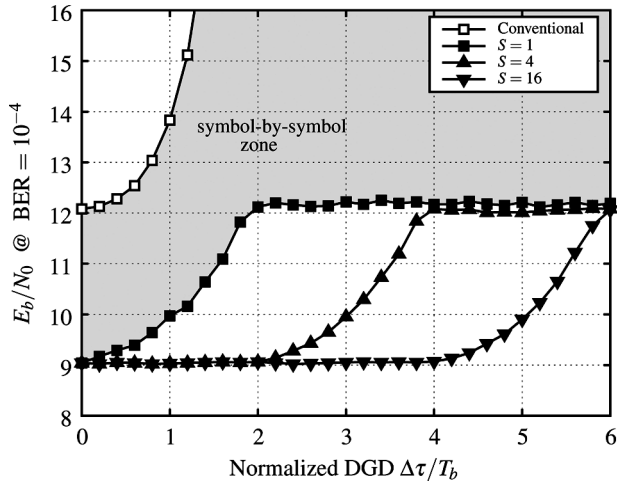


Fig. 9. Values of E_b/N_0 necessary to obtain a BER of 10^{-4} versus the value of $\Delta\tau/T_b$, when first-order PMD only is present. The considered modulation format is a QPSK.

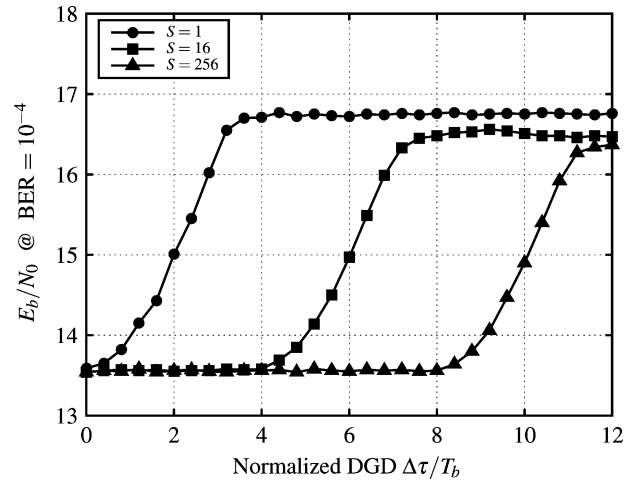


Fig. 11. Values of E_b/N_0 necessary to obtain a BER of 10^{-4} versus the value of $\Delta\tau/T_b$, when first-order PMD only is present. The considered modulation format is a 16-QAM.

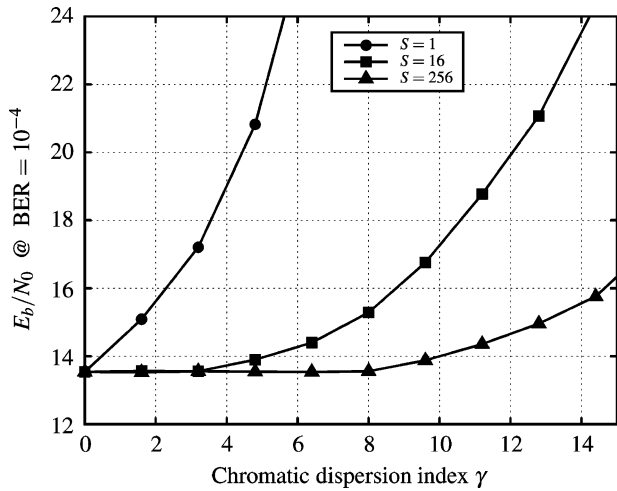


Fig. 10. Values of E_b/N_0 necessary to obtain a BER of 10^{-4} versus the value of γ , when GVD only is present. The considered modulation format is a 16-QAM.

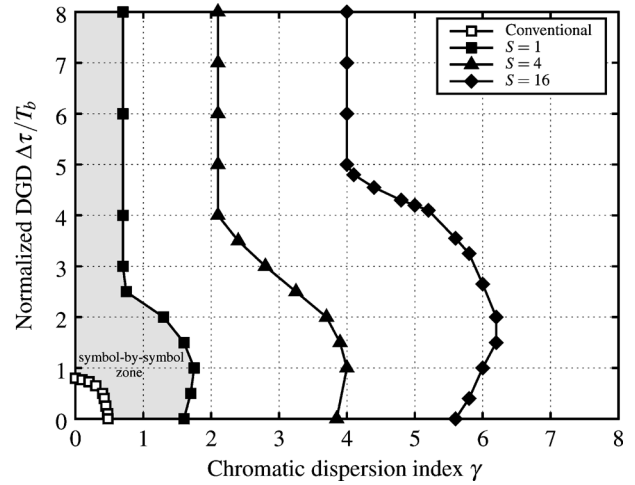


Fig. 12. Contour curves corresponding to an E_b/N_0 penalty of -4 dB for a BER = 10^{-4} , versus $\Delta\tau/T_b$ and γ . The QPSK modulation is considered.

penalty is limited to at most 3 dB. This is due to the following reason. The receiver with polarization diversity is able to perfectly resolve the slow and fast PSP in the first-order PMD approximation. When the number of trellis states is not sufficient to describe the ISI associated to the slow PSP, this PSP is perfectly canceled out by decision feedback implicit in the RSSD technique. Hence, half of the received signal power is canceled out, thus producing the 3-dB loss. In general, when a different power splitting is observed, the loss is lower, that is $\rho = 0.5$ is the worst case. In any case, this asymptotic loss can be predicted by considering the amount of power canceled out. A similar behaviour is observed in the case of a 16-QAM constellation, as can be seen in Fig. 10, referring to the case of GVD only, and in Fig. 11 devoted to the case of first-order PMD only.

Finally, in Fig. 12, the robustness of the proposed receivers to GVD and first-order PMD (with $\rho = 0.5$) is reported by showing the contour curves corresponding to an E_b/N_0 penalty of 4 dB with respect to the back-to-back case and for a BER of 10^{-4} . As can be observed, the improvement with respect to

the conventional receiver is impressive. In addition, irrespective of the number of adopted trellis states, there is a given amount of chromatic dispersion that is always tolerated for any amount of instantaneous DGD. This is due to the already observed property that, in the proposed receivers, the PMD produces a loss of at most 3 dB. Moreover, the proposed receivers show the interesting property that small values of DGD can even improve the robustness against GVD, as it was observed for duobinary modulation in [39].

VII. CONCLUSION

The use of multilevel modulations, such as phase-shift keying and quadrature amplitude modulations, in optical transmission systems has been analyzed in the presence of polarization mode dispersion and group velocity dispersion. Receiver structures, with a proper electronic processing based on the Viterbi algorithm, have been proposed which, provided that a sufficient number of trellis states is employed, achieve perfect compensation. Hence, the performance of the back-to-back case can be attained. The aspects related to the receiver implementation have

been also discussed. In particular, a couple of front end processing, both characterized by receive polarization diversity, can be employed and the algorithms to be used for channel estimation purposes have been also described. The proposed receivers can be employed not only to compensate the dispersion effects but also to separate the transmitted signals when polarization multiplexing is employed at the transmitter.

REFERENCES

- [1] J. G. Proakis, *Digital Communications*, 4th ed. New York: McGraw-Hill, 2001.
- [2] T. Foggi, E. Forestieri, G. Colavolpe, and G. Prati, "Maximum likelihood sequence detection with closed-form metrics in OOK optical systems impaired by GVD and PMD," *J. Lightw. Technol.*, vol. 24, no. 8, pp. 3073–3087, Aug. 2006.
- [3] S. Walklin and J. Conradi, "Multilevel signaling for increasing the reach of 10 Gb/s lightwave systems," *J. Lightw. Technol.*, vol. 17, no. 11, pp. 2235–2248, Nov. 1999.
- [4] R. A. Griffin and A. C. Carter, "Optical differential quadrature phase-shift key (oDQPSK) for high capacity optical transmission," in *Proc. Optical Fiber Commun. Conf.*, Anaheim, CA, Feb. 2002, pp. 367–368.
- [5] A. H. Gnauck and P. J. Winzer, "Optical phase-shift-keyed transmission," *J. Lightw. Technol.*, vol. 23, no. 1, pp. 115–130, Jan. 2005.
- [6] S. Hayase, N. Kikuchi, K. Sekine, and S. Sasaki, "Proposal of 8-state per symbol (binary ask and QPSK) 30-Gbit/s optical modulation/demodulation scheme," in *Proc. Eur. Conf. Optical Commun.*, Sep. 2003, pp. 1008–1009, paper Th.2.6.4.
- [7] M. Ohm and J. Speidel, "Optimal receiver bandwidths, bit error probabilities and chromatic dispersion tolerance of 40 Gbit/s optical 8-DPSK with NRZ and RZ impulse shaping," presented at the Proc. Optical Fiber Commun. Conf., Anaheim, CA, Mar. 2005, paper OFG5.
- [8] L. G. Kazowsky, S. Benedetto, and A. Willner, *Optical Fiber Communication Systems*. Norwood, MA: Arctec House, 1996.
- [9] G. P. Agrawal, *Fiber-Optic Communications Systems*, 3rd ed. New York: Wiley, 2002.
- [10] S. Calabró, D. van den Borne, S. L. Jansen, G. D. Khoe, and H. de Waardt, "Improved detection of differential phase shift keying through multi-symbol phase estimation," in *Proc. European Conf. Optical Commun.*, Sep. 2005, vol. 3, pp. 737–738, paper We4.P.118.
- [11] M. Nazarathy and E. Simony, "Multichip differential phase encoded optical transmission," *IEEE Photon. Technol. Lett.*, vol. 17, no. 5, pp. 1133–1135, May 2005.
- [12] X. Liu, "Receiver sensitivity improvement in optical DQPSK and DQPSK/ASK through data-aided multi-symbol phase estimation," presented at the Proc. Eur. Conf. Optical Commun., Sep. 2006, paper We2.5.6, unpublished.
- [13] D. Divsalar and M. Simon, "Multiple-symbol differential detection of MPSK," *IEEE Trans. Commun.*, vol. 38, no. 3, pp. 300–308, Mar. 1990.
- [14] F. Edbauer, "Bit error rate of binary and quaternary DPSK signals with multiple differential feedback detection," *IEEE Trans. Commun.*, vol. 40, no. 3, pp. 457–460, Mar. 1992.
- [15] H. Leib, "Data-aided noncoherent demodulation of DPSK," *IEEE Trans. Commun.*, vol. 43, no. 2–4, pp. 722–725, Feb./Mar./Apr. 1995.
- [16] G. Colavolpe and R. Raheli, "Noncoherent sequence detection," *IEEE Trans. Commun.*, vol. 47, no. 9, pp. 1376–1385, Sep. 1999.
- [17] R. Schober and W. H. Gerstacker, "Metric for noncoherent sequence estimation," *IEE Electron. Lett.*, vol. 35, no. 25, pp. 2178–2179, Nov. 1999.
- [18] W. J. Weber, "Differential encoding for multiple amplitude and phase shift keying systems," *IEEE Trans. Commun.*, vol. 26, no. 3, pp. 385–391, Mar. 1978.
- [19] G. P. Agrawal, *Nonlinear Fiber Optics*, 3rd ed. San Diego, CA: Academic, 2001.
- [20] A. F. Elrefaie, R. E. Wagner, D. A. Atlas, and D. G. Daut, "Chromatic dispersion limitations in coherent lightwave transmission systems," *J. Lightw. Technol.*, vol. 6, no. 5, pp. 704–709, May 1988.
- [21] E. Forestieri and L. Vincetti, "Exact evaluation of the Jones matrix of a fiber in the presence of polarization mode dispersion of any order," *J. Lightw. Technol.*, vol. 17, no. 12, pp. 1898–1909, Dec. 2001.
- [22] E. Forestieri and G. Prati, "Exact analytical evaluation of second-order PMD impact on the outage probability for a compensated system," *J. Lightw. Technol.*, vol. 22, no. 4, pp. 988–996, Apr. 2004.
- [23] E. Forestieri, G. Colavolpe, and G. Prati, "Novel MSE adaptive control of optical PMD compensators," *J. Lightw. Technol.*, vol. 20, no. 12, pp. 1997–2003, Dec. 2002.
- [24] H. Meyr, M. Oerder, and A. Polydoros, "On sampling rate, analog prefiltering, and sufficient statistics for digital receivers," *IEEE Trans. Commun.*, vol. 42, no. 12, pp. 3208–3214, Dec. 1994.
- [25] M. Peleg and S. Shamai (Shitz), "On the capacity of the blockwise incoherent MPSK channel," *IEEE Trans. Commun.*, vol. 46, no. 5, pp. 603–609, May 1998.
- [26] G. Colavolpe and R. Raheli, "The capacity of the noncoherent channel," *Eur. Trans. Telecommun.*, vol. 12, no. 4, pp. 289–296, Jul./Aug. 2001.
- [27] R. Nuriyev and A. Anastasopoulos, "Capacity and coding for the block-independent noncoherent AWGN channel," *IEEE Trans. Inf. Theory*, vol. 51, no. 3, pp. 866–883, Mar. 2005.
- [28] G. D. Forney, Jr., "The Viterbi algorithm," *Proc. IEEE*, vol. 61, no. 3, pp. 268–278, Mar. 1973.
- [29] G. Colavolpe and R. Raheli, "Theoretical analysis and performance limits of noncoherent sequence detection of coded PSK," *IEEE Trans. Inf. Theory*, vol. 46, no. 4, pp. 1483–1494, Jul. 2000.
- [30] R. Raheli, A. Polydoros, and C.-K. Tzou, "Per-survivor processing: A general approach to MLSE in uncertain environments," *IEEE Trans. Commun.*, vol. 43, no. 1, pp. 354–364, Feb./Apr. 1995.
- [31] M. V. Eyuboğlu and S. U. Qureshi, "Reduced-state sequence estimation with set partitioning and decision feedback," *IEEE Trans. Commun.*, vol. 38, no. 1, pp. 13–20, Jan. 1988.
- [32] A. Duel-Hallen and C. Heegard, "Delayed decision feedback estimation," *IEEE Trans. Commun.*, vol. 37, no. 5, pp. 428–436, May 1989.
- [33] P. R. Chevillat and E. Eleftheriou, "Decoding of trellis-encoded signals in the presence of intersymbol interference and noise," *IEEE Trans. Commun.*, vol. 36, no. 7, pp. 669–676, Jul. 1989.
- [34] R. Schober and W. H. Gerstacker, "Noncoherent adaptive channel identification algorithms for noncoherent sequence estimation," *IEEE Trans. Commun.*, vol. 49, no. 2, pp. 229–234, Feb. 2001.
- [35] L. R. Bahl, J. Cocke, F. Jelinek, and J. Raviv, "Optimal decoding of linear codes for minimizing symbol error rate," *IEEE Trans. Inf. Theory*, vol. 20, no. 3, pp. 284–287, Mar. 1974.
- [36] G. Colavolpe, G. Ferrari, and R. Raheli, "Noncoherent iterative (turbo) detection," *IEEE Trans. Commun.*, vol. 48, no. 9, pp. 1488–1498, Sep. 2000.
- [37] G. Colavolpe, "On LDPC codes over channels with memory," *IEEE Trans. Wireless Commun.*, vol. 5, no. 7, pp. 1757–1766, Jul. 2006.
- [38] B. F. Jorgensen, B. Mikkelsen, and C. J. Mahon, "Analysis of optical amplifier noise in coherent optical communication systems with optical image rejection receivers," *J. Lightw. Technol.*, vol. 10, no. 5, pp. 660–671, May 1992.
- [39] N. Kaneda, X. Liu, Z. Zheng, X. Wei, M. Tayahi, M. Movassaghi, and D. Levy, "Improved polarization-mode-dispersion tolerance in duobinary transmission," *IEEE Photon. Technol. Lett.*, vol. 15, no. 7, pp. 1005–1007, Jul. 2003.

Giulio Colavolpe (S'96–M'00) was born in Cosenza, Italy, in 1969. He received the Dr.Eng. degree in telecommunications engineering (cum laude) from the University of Pisa, Pisa, Italy, in 1994, and the Ph.D. degree in information technologies from the University of Parma, Parma, Italy, in 1998.

Since 1997, he has been at the University of Parma, where he is now an Associate Professor of telecommunications. In 2000, he was Visiting Scientist at the Institut Eurécom, Valbonne, France. His main research interests include digital transmission theory, adaptive signal processing, channel coding, and information theory. His research activity has led to several scientific publications in leading international journals and conference proceedings and a few industrial patents. He is also the coauthor of the book *Detection Algorithms for Wireless Communications, with Applications to Wired and Storage Systems* (Wiley, 2004).

Dr. Colavolpe received the best paper award at the 13th International Conference on Software, Telecommunications, and Computer Networks (SoftCOM 2005). He is also the principal investigator of several research projects funded by the European Space Agency (ESA-ESTEC) and important telecommunications companies.

Tommaso Foggi was born in Parma, Italy, on May 7, 1978. He received the Dr. Ing. degree in telecommunications engineering from the University of Parma in April 2003. He is currently pursuing the Ph.D. degree at the Dipartimento di Ingegneria dell'Informazione (DII), University of Parma.

From July 2003 to July 2004, he was granted a CNIT scholarship at Photonic Networks National Laboratory, Pisa, Italy, and then another CNIT scholarship from July 2005 to July 2006 at Dipartimento di Ingegneria dell'Informazione (DII), Università Degli Studi di Parma, Parma. His main research interests include electrical compensation of impaired optical transmission systems and satellite navigation and positioning.

Enrico Forestieri (S'91–M'92) was born in Milazzo, Italy, in 1960. He received the Dr. Ing. degree in electronics engineering from the University of Pisa, Pisa, Italy, in 1988.

From 1989 to 1991, he was a postdoctoral scholar at the University of Parma, Parma, Italy, working on optical communication systems. From 1991 to 2000, he was a Research Scientist and faculty member of the University of Parma. Since 2001, he has been with the Scuola Superiore Sant'Anna di Studi Universitari e di Perfezionamento, Pisa, where he is currently a Professor of telecommunications. His research interests are in the general area of digital communication theory and optical communication systems, with special attention on adaptive optical and electronic equalization, channel coding, and advanced modulation formats for optical systems. He is the Leader of the "Optical Transmission Theory and Techniques" area at the Integrated Research Center for Photonic Networks and Technologies (IRCPhoNeT), Pisa. His research activity has led to numerous scientific publications in leading international journals and conference proceedings, as well as a few patents.

Dr. Forestieri was the General Chairman of the Tyrrhenian International Workshop on Digital Communications in 2004.

Giancarlo Prati (M'81–F'03) was born in Rome, Italy, on November 13, 1946. He received the Dr. Ing. degree (*cum laude*) in electronics engineering from the University of Pisa, Pisa, Italy, in 1972.

From 1975 to 1978, he was an Associate Professor of electrical engineering at the University of Pisa. From 1978 to 1979, he was on a NATO-supported Fellowship Leave in the Department of Electrical Engineering, University of Southern California, Los Angeles, working in optical communications. In 1982, he was Visiting Associate Professor with the Department of Electrical and Computer Engineering, University of Massachusetts, Amherst. From 1976 to 1986, he was a Research Scientist of the Italian National Research Council (CNR) at the Centro di Studio per Metodi e Dispositivi di Radiotrasmissione, Pisa. From 1986 to 1988, he was Professor of Electrical Engineering at the University of Genoa, Italy. From 1988 to 2000, he was a Professor of telecommunications engineering at the University of Parma, Parma, Italy, where he served as Dean of the Engineering Faculty from 1992 to 1998. He is now a Professor of telecommunications at the Scuola Superiore Sant'Anna, Pisa, Italy. His professional and academic interests are in telecommunication systems and digital signal processing in communications. The activity has focused on optical communications and radiofrequency communications, with applications to satellite communications, high-capacity terrestrial digital radio links, mobile radio, modems for switched telephone lines, and fiber communications.

Dr. Prati is currently the President of CNIT, Italian Interuniversity Consortium for Telecommunications, incorporating 35 Universities. From 1997 to 2006, he was a member of the Technical Program Committee of the European Conference on Optical Communications (ECOC).